Biochimica et Biophysica Acta, 943 (1988) 95–102
Elsevier

BBA 74073

Conformational analysis of lipid-associating proteins in a lipid environment

R. Brasseur [a], H. De Loof [b], J.M. Ruysschaert [a] and M. Rosseneu [b]

[a] *Laboratoire des Macromolecules aux Interfaces, Free University Brussel., Brussels and* [b] *Department Clinical Biochemistry, A.Z. St-Jan, 8000 Brugge (Belgium)*

(Received 29 October 1987)
(Revised manuscript received 18 April 1988)

Key words: Lipid binding; Conformational analysis; Helical structure; Computer model

Two major types of helical structures have been identified in lipid-associating proteins, being either amphipathic or transmembrane domains. A conformational analysis was carried out to characterize some of the properties of these helices. These calculations were performed both on isolated helices and in a lipid environment. According to the results of this analysis, the orientation of the line joining the hydrophobic and hydrophilic centers of the helix seems to determine the orientation of the helix at the lipid/water interface. The calculation of this parameter should be useful to discriminate between an amphipathic helix, parallel to the interface and a transmembrane helix orientated perpendicularly. The membrane-spanning helices are completely immersed in the phospholipid bilayer and their length corresponds to about the thickness of the hydrophobic core of the DPPC bilayer. The energy of interaction, expressed per phospholipid is significantly higher for the transmembrane compared to the amphipathic helices. For the membrane-spanning helices the mean energy of interaction is higher than the interaction energy between two phospholipids, while it is lower for most amphipathic helices. This might account for the stability of these protein-anchoring domains. This computer modeling approach should usefully complement the statistical analysis carried out on these helices, based on their hydrophobicity and hydrophobic moment. It represents a more refined analysis of the domains identified by the prediction techniques and stress the functional character of lipid-associating domains in membrane proteins as well as in soluble plasma lipoproteins.

Introduction

Helical domains are common both in water-soluble and in membrane-associated proteins [1,2]. Based on their hydrophobicity and on their helical hydrophobic moment, Eisenberg et al. [2] proposed a classification of these helices in terms of 'globular', 'surface-seeking' and 'membrane-spanning' domains. The surface-seeking helices have a moderate hydrophobicity and a high helical hydrophobic moment, while the membrane-spanning helices have a high hydrophobicity and relatively low helical moment.

Plasma apolipoproteins have a high helical content which increases upon their association with phospholipids [3]. These lipid-association properties have been attributed to the presence of amphipathic helices, as first proposed by Segrest et al. [5]. A large body of evidence, accumulated over the last decade, supports this original hypothesis [6]. The amphipathic helix model is defined by an arrangement of amino acid residues which results in domains with a helicoidal secondary structure containing opposing polar and hydrophobic faces.

Correspondence: M. Rosseneu, Department of Clinical Biochemistry, A.Z. St-Jan, 8000 Bruges, Belgium.

The association of apolipoproteins and phospholipids is driven by the exclusion of apolar amino acids from the aqueous phase. Within the apolipoproteins, positively charged amino acids occur mostly at the polar/non-polar interface while negatively charged amino acids are located at the center of the hydrophilic side of the helix [5,6]. A specific role of the charged residues has also been proposed [5]. The acyl chains of the positively charged arginine and lysine residues could contribute to the hydrophobicity of the apolar face. The ionic interactions between the opposite charges within the helix and/or the ionic interaction with the zwitterionic phospholipids may play a role in the initiation, the stability or the substrate properties towards enzymes, of the apolipoprotein-phospholipid complexes [7].

Some peptides such as calcitonin [8], or domains of other proteins, such as *sn*-1,2-diacylglycerol kinase [9] can also form amphipathic helices. The amphipathic helix hypothesis has also been tested by different groups using various synthetic peptides, analogous to apolipoprotein domains [10–14].

Membrane-spanning helices have been identified in several integral membrane proteins and especially in cellular receptors present at the cell surface [15–24]. These proteins include: the receptor for low-density lipoprotein (LDL-R) [15], for growth factors such as the epidermal growth factor (EGF-R) [16] and the platelet-derived growth factor (PDGF-R) [17], for tyrosine kinase [18], human insulin (HI-R) [19], human transferrin (HT-R) [20] and the receptor for the transepithelial transport of IgA and IgM (IGAM-R) [21], the asialoglycoprotein receptor [22] and viral proteins such as the vesicular stomatitis virus protein (VSVP) [23] and the protein product of the v-*fms* gene (FMS) [24]. The transmembrane domains of these proteins have an helical structure consisting almost exclusively of hydrophobic amino acids and encompassing between 20 and 28 residues, sufficient to span the phospholipid bilayer [23]. These regions function as anchors for the proteins at the cell surface [16].

Since the sequences of the amphipathic helices are made of both polar and apolar residues it can be expected that their interactions with lipids, in terms of energy of association and mutual orientation will be specific for each class of helix.

The aim of the work described in this paper is to carry out a conformational analysis of these two types of lipid-associating helices and to relate the results of the computer modeling to some of the characteristic properties of these helical structures.

Computational methodology

The computer aided modeling procedure is carried out as follows [25]: (A) imposing a helical structure to the peptide, based upon the Garnier prediction for the secondary structure [26]; (B) orienting this structure at a water-lipid interface; (C) surrounding the oriented peptide with phospholipid molecules and (D) calculating the interaction parameters of the peptide-lipid complex generated by the computer.

Protein domains were imposed a secondary structure according to the torsional angles corresponding to the alpha-helical structure and this was maintained throughout the assembly procedure. The peptide was oriented at the air/water interface as described earlier [25] and its position was also maintained. In this procedure the peptide is oriented with the line joining the hydrophilic and hydrophobic centers perpendicular to the interface (Fig. 1).

The hydrophilic center ($\vec{C}^{\text{phi}}$) is defined by the following equation:

$$\vec{C}^{\text{phi}} = \frac{\sum_{i=1}^{n} E^{+}_{tr_i} \cdot \vec{r}_i}{\sum_{i=1}^{n} E^{+}_{tr_i}}$$

in which $\vec{r}_i$ are the coordinates of the ith atom. The hydrophobic center located in the hydrocarbon domain ($\vec{C}^{\text{pho}}$) is defined by the same equation, except that the negative transfer energies (E_{tr_i}) are taken into account. The interface position ($\vec{I}$) is defined by the equation:

$$\frac{\sum_{i=1}^{n} E^{+}_{tr_i}}{\vec{C}^{\text{phi}} - \vec{I}} = \frac{\sum_{j=1}^{m} E^{-}_{tr_j}}{\vec{C}^{\text{pho}} - \vec{I}}$$

The procedure used to surround the peptide with phospholipids is a modification of the method

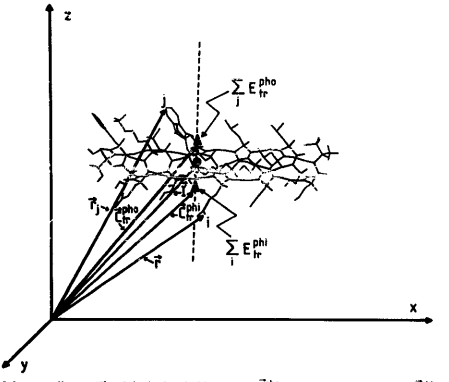

Fig. 1. Definition of the co-ordinates ($\vec{r}_i$) of the hydrophobic center ($\vec{C}^{pho}_{tr}$), the hydrophilic center ($\vec{C}^{phi}_{tr}$) and the interface $\vec{r}$.

previously applied to pharmacological agents and other small molecules [27,28]. A phospholipid molecule was moved along the *X*-axis in steps of 0.05 nm. For each position the lipid was rotated in steps of 30° around its long axis *Z'* and around the amphipathic helix. *l* is the number of positions along the *X*-axis, *m* the number of rotations of the second molecule around the first one and *n* is the number of rotations of the lipid itself. For each set of values of *l*, *m* and *n*, the intermolecular interaction energy was calculated as the sum of the London-Van der Waals, the electrostatic energy and the transfer energy for atoms, or groups of atoms, from a hydrophobic to a hydrophilic phase.

In a following step, the phospholipid was allowed to move along the *Z'*-axis perpendicular to the interface and the position of the *Z'*-axis was varied with respect to the *Z*-axis, in order to obtain the lowest interaction energy state for each set of values *l*, *m* and *n*. This energy and the coordinates associated to each *l*, *m* and *n* combination, were stored in a hyper matrix in decreasing order of the interaction energy. The assembly procedure was then carried on with additional phospholipids. The orientation of the second phospholipid is the next energetically favorable orientation stored in the hyper matrix while taking into account the steric and energetic constraints imposed by the presence of the phospholipids already assembled. Thus, orientations are disregarded in which overlaps of atomic coordinates of two molecules occur and in which the interaction energies between the two molecules were positive.

Subsequently, the positions of the first and second phospholipid are alternatively modified according to the energy classification of the hyper matrix in order to further minimize the conformation energy. For the third lipid, the same process is repeated but now the positions of the three surrounding lipids are modified alternatively in order to find the lowest energy state. The assembly procedure is completed when the helix is surrounded by the number of first lipid neighbors. For the transmembrane helices, these calculations are first carried out on one half of the helix, and an identical procedure is used to surround the second half of the peptide with the first lipid neighbors in the second monolayer. The interac-

tion energies between the helices and crystalline dipalmitoylphosphatidylcholine (DPPC) were calculated as described before [29].

All calculations were performed on an Olivetti M28 using a 80287 processor and the PC-TAMMO procedure (theoretical analysis of molecular membrane organization) as extensively described [30]. Graphs were drawn with the PC-MGM (molecular graphics manipulation) program.

Results and Discussion

For the analysis of the membrane-spanning helices we restricted ourselves to the membrane proteins where a single membrane-spanning domain had been identified. Protein-protein interactions between adjacent helices such as in rhodopsin or in channel-forming proteins [1] are therefore not included in the calculations. In the selected proteins, the membrane-spanning domain was mostly identified by calculation of the hydrophobicity profile throughout the sequence [15,19]. The introduction of deletions and mutations in these domains, through genetic engineering [31], further validated the predictive calculations.

The amphipathic helices selected for the calculations belong to either natural proteins such as human, porcine or salmon calcitonin [8], plasma apolipoprotein AI [10], *sn*-1,2-diacylglycerol kinase of *Escherichia coli* [9], or to synthetic peptides. These peptides have been designed to experimentally test the contribution of amphipathic helices to the lipid-binding properties of apolipoproteins and include the LAP16, LAP20, LAP24 series [11] as well as the PI, 18A, 18R and 17desA peptides [10,13–14].

The sequences of the 12 amphipathic and 10 transmembrane helices are summarized in Table I. The membrane-spanning helix of the asialoglycoprotein receptor (ASGL-R) and the amphipathic LAP20 peptide are depicted in an Edmundson wheel representation in Fig. 2. This figure illustrates the pronounced hydrophobic character of the transmembrane helix and the segregation of the polar and apolar residues in the amphipathic helix.

TABLE I

SEQUENCES OF THE 12 AMPHIPATHIC AND 10 MEMBRANE-SPANNING HELICES

Peptide	Ref.	Sequence
Hum. calcitonin (hCT)	8	CGNLSTCMLGTYTQDFNKFHTFPQTAIGVGAP
Porc. calcitonin (pT)	8	CSNLSTCVLSAYWRNLNNFHRFSGMGFGPETP
Salm. calcitonin (sCT)	8	CSNLSTCVLGKLSQELHKLQTYPRTNTGSGTP
DKinase (74–92)	9	SAIEAVVDRIGSEYHELSG
Apo AI (198–219)	10	PKLEELKEKRKELLEKLKEKLA
Peptide I	10	LLQSLLSLLQSLLSLLLQWLKRKRQQ
LAP 16	11	VSSLKEYWSSLKESFS
LAP 20	11	VSSLLSSLKEYWSSLKESFS
LAP 24	11	VSSLLSSLLSSLKEYWSSLKESFS
18A	13,14	DWLKAFYDKVAEKLKEAF
18R	13,14	KWLDAFYKDVAKELKEAF
17 DES A	13,14	DWLKAFYDKAEKLKEAF
Low Density Lipoprotein Rec. (LDL-R)	15	ALSIVLPIVLLVFLCLGVFLLWK
Epidermal Growth Factor Rec. (EGF-R)	16	TFIIATVEGVLLFLILVVVVGILI
Platelet-der. Growth. Fac. Rec. (PDGF-R)	17	VVVISAILALVVLTVISLIILIML
Tyrosine Kinase Receptor (TK-R)	18	IVSAVVGILLVVVLGVVFGILI
Human Insulin Receptor (HI-R)	19	IIIGPLIFVFLFSVVIGSIYLFL
Human Transferrin Receptor (HT-R)	20	CSGSICYGTIAVIVFFLIGFMIGYL
IgA&M Tr. Epithel. Transp. Rec. (IGAM-R)	21	VLISTLVPLGLVLAAGAMAVAIA
Asialoglycoprotein Receptor (ASGL-R)	22	FAAVYVLLALSFLLLTLLSSVSL
Vesicul. Smotatitis Virus Prot. (VSVP)	23	SSIASFFFIIGLIIGLFLVL
V-FMS Virus Protein (FMS)	24	FLFTPVVVACMSIMALLLLLLLLLL

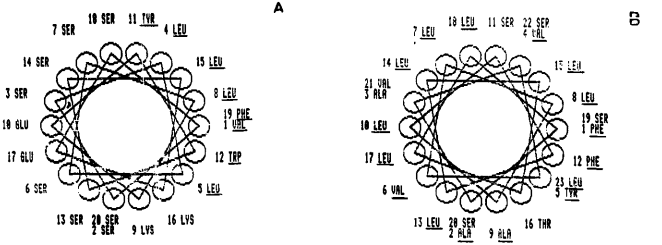

Fig. 2. Edmundson-wheel diagram of the amphipathic LAP 20 peptide (A) and the transmembrane asialoglycoprotein receptor ASGL-R peptide (B) showing the segregation of the apolar (underlined) and polar residues in the amphipathic peptide and the hydrophobic character of the membrane-spanning peptide.

The computer modeling analysis yields some characteristic parameters for these helices such as the hydrophobic and hydrophilic transfer energies from water to a lipid phase, the distance between hydrophobic and hydrophilic centers and the hydrophobic-hydrophilic balance (Table II). The results stress the opposite character of the two classes of helices. In the membrane-spanning helices, the hydrophobic energy of transfer is significantly higher than the hydrophilic contribution. This results in a positive hydrophobic to hydrophilic balance, whereas the reverse is observed with the amphipathic helices. The distance between hydrophobic and hydrophilic centers is similar for all helices and varies between 0.8 and 2.3 Å. Their orientation is however opposite, as the line joining the hydrophobic and hydrophilic centers is oriented perpendicular to the axis of the amphipathic helix, while it lies parallel to the axis of a transmembrane helix (Figs. 3 and 4). Experimental evidence supporting the calculated orientation of the LAP-20 peptide synthesized by Pownall et al. [11] and that of similar peptides was presented by Anantharamaiah et al. [13,14]. We carried out infra-red measurements with polarized light of the LAP-20 peptide interacting with DMPC. The angle obtained between the phospholipid bilayer and the peptide chain supports the theoretical model

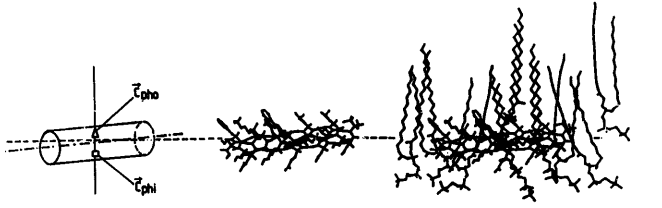

Fig. 3. Representation of the properties and mode of insertion of the amphipathic LAP 20 peptide in a lipid matrix. From left to right: schematic representation of the hydrophobic ($\vec{C}_{pho}$) and hydrophilic ($\vec{C}_{phi}$) centers compared to the axis of the helix, skeleton representation of the helix and same representation of the helix surrounded by nine DPPC molecules. The dotted line corresponds to the lipid/water interface.

TABLE II

CONFORMATIONAL PARAMETERS OF THE TWELVE AMPHIPATHIC AND TEN TRANSMEMBRANE ALPHA HELICES

Hydrophobic (E_{pho}) and hydrophilic transfer energy (E_{phi}) in (kcal/mol). Hydrophobic-hydrophilic balance (Phi). Phi = $\log(E_{pho}/E_{phi})$ Distance between the hydrophobic and hydrophobic center (Delta, Å).

Peptide	E_{pho}	E_{phi}	Phi	Delta
hCT	167	160	0.019	0.96
pCT	175	177	−0.005	1.38
sCT	169	162	0.018	1.08
DKinase (74–92)	181	195	−0.032	1.24
LAP 16	174	170	0.010	1.33
LAP 20	214	205	0.019	1.42
LAP 24	254	240	0.025	1.51
Apo AI (198–219)	270	245	0.042	0.82
Peptide I	271	232	0.067	1.20
18A	213	184	0.064	1.40
18R	213	184	0.064	1.31
17 des A	202	177	0.057	1.19
LDL-R	279	176	0.198	0.82
EGF-R	277	184	0.178	1.46
PDGF-R	277	182	0.182	1.25
TK-R	239	160	0.172	1.42
HI-R	279	175	0.202	0.40
HT-R	288	230	0.098	1.89
IGAM-R	224	170	0.120	0.61
ASGL-R	256	188	0.135	0.49
VSVP	229	154	0.170	2.33
FMS	296	186	0.202	1.36

(unpublished observations). Finally the same type of calculations and of infra-red measurements was performed on the paramyxovirus F1 N-terminal peptide (18 residues) and the theoretical and experimental results were in good agreement [32].

After assembly of the two classes of helices with DPPC molecules (Figs. 3 and 4), the number of first phospholipid neighbors, the mean interaction energy per phospholipid and the angle of the axis of the helix with the lipid/water interfaces were calculated (Table III). For all parameters, significant differences appear between the two classes of helices. The transmembrane helices lie parallel to the phospholipid acyl chains (Fig. 3) while the amphipathic helices lie at an angle varying between 0° and 20° with the interface, in agreement with the model proposed for the complexes formed between phospholipids and synthetic peptides [14]. The amphipathic helices penetrate into the phospholipid monolayer up to a distance corresponding to about the 4th carbon atom of the acyl chains, in agreement with experimental data obtained by NMR on apolipoprotein-phospholipid interactions [3]. The membrane-spanning helices are completely immersed in the phospholipid bilayer and their length corresponds to about the thickness of the hydrophobic core of the DPPC bilayer [1]. The energy of interaction, expressed per phospholipid is significantly higher for the transmembrane compared to the amphipathic helices. For the membrane-spanning helices the mean energy of interaction is higher than the interaction energy between two phospholipids

TABLE III

INTERACTION PARAMETERS BETWEEN THE ALPHA HELICES AND DPPC

Mean energy of interaction between one phospholipid molecule and the helical peptide (E_{int}, kcal/mol phospholipid), number of phospholipid neighbors (number of lipids) in the 1st and 2nd layer, orientation of the helix at the lipid water interface (angle).

	E_{int}	Number of lipids		Angle (°)
		1st layer	2nd layer	
hCT	−12.5	8	/	0
pCT	−11.6	6	/	10
sCT	−12.2	5	/	25
DKinase (72–92)	−10.5	7	/	20
LAP 16	−11.7	9	/	0
LAP 20	−12.6	9	/	5
LAP 24	−10.4	7	/	0
Apo AI (198–219)	−12.7	8	/	20
Peptide I	−14.4	8	/	10
18 A	−19.6	7	/	0
18R	−12.3	8	/	−5
17 DES A	−12.5	6	/	0
LDL-R	−18.06	4	7	90
EGF-R	−21.83	8	5	85
PDGF-R	−13.33	8	6	90
TK-R	−19.33	8	6	85
HI-R	−17.54	9	4	85
HT-R	−16.60	7	5	90
IGAM-R	−14.60	7	5	90
ASGL	−25.46	9	5	83
VSVP	−29.60	8	5	90
FMS	−25.46	5	9	85

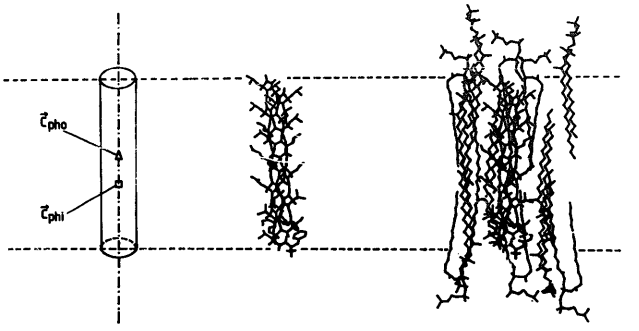

Fig. 4. Same representation for the asialoglycoprotein receptor (ASGL-R) spanning the DPPC bilayer. Dotted lines indicate the two interfaces of the bilayer.

(−13 kcal/mol) in a pure phospholipid bilayer, while it is lower for most amphipathic helices. This might account for the stability of these protein-anchoring domains, compared to the transfer properties of most plasma apolipoproteins among lipoproteins [6].

In conclusion, this conformational analysis method, applied to different types of helical segments existing in lipid-associating proteins, enables the computation of the parameters accounting for the different properties of such helices. According to the results of this analysis, the orientation of the line joining the hydrophobic and hydrophilic centers of the helix seems to determine the orientation of the helix at the lipid/water interface. The calculation of this parameter should be useful to discriminate between an amphipathic helix, parallel to the interface and a transmembrane helix orientated perpendicularly.

The representation of these segments at the molecular level and the visualization of their orientation in a phospholipid environment facilitates the comprehension of their mechanism of insertion into a lipid layer. This computer modeling approach should usefully complement the statistical analysis carried out on these helices, based on their hydrophobicity and hydrophobic moment [2,33]. It represents a more refined analysis of the domains identified by the prediction techniques and stress the functional character of lipid-associating domains in membrane proteins as well as in soluble plasma lipoproteins.

Acknowledgement

R. Brasseur is a Qualified Researcher of the Belgian National Fund for Scientific Research.

References

1 Engleman, D.M., Steitz, T.A. and Goldman, A. (1986) Annu. Rev. Biophys. Chem. 15, 321–353.
2 Eisenberg, D., Weiss, R.M. and Terwilliger, T.C. (1982) Nature 299, 371–374.
3 Sparrow, J.T. and Gotto, A.M. (1981) CRC Crit. Rev. Biochem. 13, 87–107.
4 Eisenberg, D., Weiss, R.M. and Terwilliger, T.C. (1984) Proc. Natl. Acad. Sci. USA 81, 140–144.
5 Segrest, J.P., Jackson, R.L., Morrisett, J.D. and Gotto, A.M. (1973) FEBS Lett. 38, 247–253.
6 Massey, J.B. and Pownall, H.J. (1986) Methods. Enzymol. 128, 403–413.
7 De Loof, H., Rosseneu, M., Brasseur, R. and Ruysschaert, J.M. (1987) Biochim. Biophys. Acta 911, 45–52.
8 Epand, R.M., Epand, R.F., Ormlowski, R.C., Schueter, R.J., Boni, L.T. and Hui, S.W. (1983) Biochemistry 22, 5074–5084.

9 Loomis, R., Walsh, P. and Bell, R.M. (1985) J. Biol. Chem. 260, 4091–4097.
10 Fukushima, D., Yokoyama, S., Kezdy, F.J. and Kaiser, E.T. (1981) Proc. Natl. Acad. Sci. USA 78, 2732–2736.
11 Pownall, H.J., Gotto, A.M. and Sparrow, J.T. (1984) Biochim. Biophys. Acta 793, 149–156.
12 Pownall, H.J., Knapp, R.D., Gotto, A.M. and Massey, J.B. (1983) FEBS Lett. 159, 17–23.
13 Anantharamaiah, G.M., Jones, J.L., Brouillette, C.J., Schmidt, C.F., Chung, B.H., Hughes, T.A., Brown, A.S. and Segrest, J.P. (1986) J. Biol. Chem. 260, 10248–10255.
14 Anantharamaiah, G.M. (1986) Methods Enzymol. 128, 627–647.
15 Yamamoto, T., Davis, C.G., Brown, M.S., Schneider, W.J., Casey, M.L., Goldstein, J.L. and Russel, D.W. (1984) Cell 9, 27–36.
16 Bargman, C.I., Hung, M.C. and Weinberg, R.A. (1986) Nature 319, 227–230.
17 Yarden, Y., Escobedo, J.A., Kuang, W.-J., Yang-Feng, T.L., Daniel, T.O., Tremble, P.M., Chen, E.Y., Ando, M.E., Harkins, R.N., Francke, U., Fried, V.A., Ullrich, A. and Williams, L.T. (1986) Nature 323, 226–232.
18 Coussens, L., Yang-Feng, T.L., Liao, Y.C., Chen, E., Gray, A., McGrath, J., Seeburg, P.H., Libermann, T.A., Schlessinger, J., Francke, U., Levinson, A. and Ullrich, A. (1986) Science 230, 1132–1139.
19 Ebina, Y., Ellis, L., Jarnagin, K., Edery, M., Graf, L., Clauser, E., Ou, J.-H., Masiarz, F., Kan, Y.W., Goldfine, I.D., Roth, R.A. and Rutter, W.J. (1985) Cell 40, 747–758.
20 McClelland, A., Kühn, L.C. and Ruddle, F.H. (1984) Cell 39, 267–274.
21 Moskov, K.E., Frielander, M. and Blobel, G. (1984) Nature 308, 37–43.
22 Drickamer, K. (1981) J. Biol. Chem. 256, 5827–5839.
23 Adams, G.A. and Rose, J.K. (1985) Cell 41, 1007–1015.
24 Coussens, L., Van Beveren, C., Smith, D., Chen, E., Mitchell, R.L., Isacke, C.M., Verma, I.M. and Ullrich, A. (1986) 320, 277–280.
25 Brasseur, R. and Ruysschaert, J.M. (1986) Biochem. J. 238, 1–11.
26 Garnier, J., Osguthorpe, D.J. and Robson, B. (1978) J. Mol. Biol. 120, 97–120.
27 Brasseur, R., Cabiaux, V., Killian, J.A., De Kruijff, B. and Ruysschaert, J.M. (1986) Biochim. Biophys. Acta 855, 317–324.
28 Brasseur, R., Killian, J.A., De Kruijff, B. and Ruysschaert, J.M. (1987) Biochim. Biophys. Acta 903, 11–17.
29 Brasseur, R., Goormaghtigh, E. and Ruysschaert, J.M. (1981) Biochem. Biophys. Res. Commun. 103, 301–310.
30 Brasseur, R. (1986) J. Mol. Graphics 4, 117–120.
31 Lehrman, M.A., Russel, D.W., Goldstein, J.L. and Brown, M.S. (1987) J. Biol. Chem. 262, 3354–3361.
32 Brasseur, R., Lorge, P., Espion, D., Goormaghtigh, E., Burny, A. and Ruysschaert, J.M. (1988) Virus Genes, in press.
33 De Loof, H., Rosseneu, M., Brasseur, R. and Ruysschaert, J.M. (1986) Proc. Natl. Acad. Sci. USA 83, 2295–2299.